

Uncertainties in the oscillation parameters measurement due to multi-nucleon effects at NO ν A Experiment

Paramita Deka^{1 *}, Jaydip Singh^{2 †}, Neelakshi Sarma¹, Kalpana Bora^{1 ‡}

*Department Of Physics, Gauhati University, Assam, India¹ and
Department Of Physics, Lucknow University, Uttar Pradesh, India²*

In this work, we investigate the role of multi-nucleon (MN) effects (mainly 2p-2h and RPA) on the sensitivity measurement of various neutrino oscillation parameters, in the disappearance channel of NO ν A (USA) experiment. Short-range correlations and detector effects have also been included in the analysis. We use the kinematical method of reconstruction of the incoming neutrino energy, both at the near and far detectors. The extrapolation technique has been used to estimate oscillated events at the far detector. The latest global best fit values of various light neutrino oscillation parameters have been used in the analysis. We find that MN effects increase uncertainty in the measurement of neutrino oscillation parameters, while lower detector efficiency is reflected in more uncertainty. This study can give useful insight into precision studies at long-baseline neutrino experiments in future measurements.

I. INTRODUCTION

Precise and adequate knowledge of neutrino scattering cross-sections and nuclear effects in them is very important to reduce the systematic uncertainties in neutrino beam oscillation experiments. The insufficiency in our present understanding of these effects inflicts the precision measurements of yet unknown neutrino oscillation parameters and some other experimentally observed anomalies in the neutrino sector. In current and future neutrino oscillation experiments [1–11] on neutrino oscillation, nuclear effects in neutrino interactions are one of the principal sources of systematic uncertainties. From the recent result of the T2K [12] appearance channel, it is observed that nuclear effects are the largest contributors among all the systematic errors. One of the main contributions to this systematic uncertainty comes from the description of nucleon correlations in the initial state which may induce 2-particle-2-hole (2p-2h) effect in the final state. Due to the presence of such interactions excess events are observed in recent neutrino experiments. The 2p-2h effect is dominated by the meson exchange current (MEC) which involves 2 nucleons, or 2-body current. Nuclear effects (due to the presence of many nucleons in the target) influence both the neutrino scattering cross-section and kinematics of the final state. Due to a poor understanding of nuclear effects in neutrino scattering, uncertainty regarding cross-section models increases. The nuclear effects include Fermi motion of the nucleons, the binding energy of the nucleon in the nucleus, Pauli blocking and final state interactions (FSIs). FSI further includes re-scattering of the outgoing particles with the nuclear remnant. Nuclear effects along with FSI bias or smear the reconstructed neutrino energy. Thus a good understanding of these effects is essential.

Long-baseline neutrino oscillation experiments usually use a two detector setup. A small near detector (ND) is placed close to the neutrino production target which constrains neutrino-nucleus interaction cross-sections and neutrino flux and is useful in reducing systematic uncertainties. To observe the neutrino oscillations, a larger far detector (FD) is installed at a larger distance. By comparing the unoscillated and the oscillated flux, the oscillation probability can be measured which later helps to calculate mixing angles, mass squared differences, etc. These experiments aim to measure the six neutrino oscillation parameters—two mass splittings - Δm_{21}^2 , Δm_{32}^2 , three mixing angles - θ_{12} , θ_{23} , θ_{13} and one CP phase δ_{CP} , and are designed to measure two channels - appearance and disappearance channels. A neutrino changes its flavor from α to β ($\nu_\alpha \rightarrow \nu_\beta$) during its journey from one detector to another and the appearance experiments measure the probability of appearance $P_{\alpha \rightarrow \beta}(E)$ of this neutrino flavor β as a function of energy at a given distance. The disappearance experiment, on the other hand, looks at the probability of disappearance $P_{\alpha \rightarrow \alpha}(E)$ of the flavour α at a given distance from the source. Out of these six neutrino oscillation parameters, four parameters θ_{12} , θ_{13} , Δm_{21}^2 and $|\Delta m_{32}^2|$ are determined precisely from the experiments, while Octant of the atmospheric mixing angle θ_{23} , leptonic CP-violating phase δ_{CP} and mass hierarchy remains to be fixed.

* E-mail: paramitadeka@gauhati.ac.in

† E-mail: jdsingh@fnal.gov

‡ kalpana@gauhati.ac.in

Ongoing T2K and NO ν A [11] experiments are expected to measure these unknown parameters. From the published data of these two experiments in 2018 and 2019 [9, 12–14], the T2K best-fit point is at $\sin^2 \theta_{23} = 0.53^{+0.03}_{-0.04}$ for both hierarchies and $\delta_{CP}/\pi = -1.89^{+0.70}_{-0.58} (-1.38^{+0.48}_{-0.54})$ for normal (inverted) hierarchy [14]. For NO ν A, the best-fit point is at $\sin^2 \theta_{23} = 0.56^{+0.04}_{-0.03}$, and $\delta_{CP}/\pi = 0^{+1.3}_{-0.4}$ for normal hierarchy. Again, as per the latest results presented at Neutrino 2020 conference, the best-fit point for NO ν A (T2K) is $\sin^2 \theta_{23} = 0.57$ (0.528) and $\delta_{CP} = 0.82\pi$ (-1.6π) for normal hierarchy [15]. This tension between the results of two experiments may be an indication of discrepancy among different models.

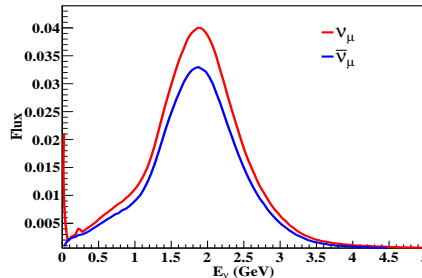


FIG. 1: NO ν A ND neutrino and antineutrino flux as a function of neutrino energy used in our work. For full experimental setup and estimates for the neutrino flux from NUMI, please see Refs. [13, 16–21].

Though sufficient work has been done to understand the role of nucleons in neutrino-scattering still more needs to be done to reduce uncertainties and improve precision. Some of the low energy baseline experiments use a kinematic method of energy reconstruction by assuming a neutron at rest in a quasi-elastic (QE) scattering. Non-QE events may be wrongly identified as QE events due to final state interactions which lead to a wrong value of the reconstructed neutrino energy lower than true incoming energy. From the MiniBooNE and K2K experiments, it came to notice that the cross-section earlier considered as QE contains about 30% contribution from 2p-2h events [24–26]. Both charged current (CC) and neutral current (NC) analyses of QE events showed an excess of cross-section than expected from QE scattering. It has been shown that in addition to pion production, any QE scattering event gets background contribution from the presence of multi-nucleon events e.g., 2p-2h excitations [26–29, 32] and all other reaction process [33] which lead to the downward shift of reconstructed energy. These uncertainties affect the reconstructed energy which further impacts the extraction of oscillation parameters. More details of these effects for MiniBooNE and T2K experiments can be found in Refs. [33–36]. Coloma et al. in [36] have shown the impact of different neutrino interactions and nuclear models in neutrino oscillation parameters determination in the ν_μ disappearance channel. A good agreement of the MiniBooNE data [25, 26] is obtained by Martini et al. by combining Random Phase Approximation (RPA) with 2p-2h contributions. RPA method is a non-perturbative method that is developed to understand the long-range correlation between nucleons inside the nucleus which gives the collective excitation of the nucleus. It is termed as "Random Phase" because the collective excitations of different phases are treated randomly. In GENIE, RPA is included using the Nieves model [37] created by Valencia group to describe the complexity of many-body interactions. This effect modifies the low-lying energy states of the nucleus by changing the potential. Simultaneously it creates a screening effect which in turn reduces the probability for an electromagnetic and weak interaction with those states. Since the probability of weak interaction is less, this results in fewer QE interactions with RPA. Hence it is observed that RPA corrections reduce the cross-sections and it affects largely at lower energies. At higher energies, the RPA reductions become smaller [37], however, RPA suppressions of about 20-30% for the higher energies can still be found. The RPA suppression also reduces with an increase in lepton effective momentum and it grows with atomic mass number A . From early works on electron scattering data, it has been shown that RPA correction plays a vital role in the peak QE region where these corrections tend to lower the cross-section [38]. Similar effects in neutrino-induced interactions are discussed by Kim et al. in Ref. [39]. In [40], RPA correlations and 2p-2h (multi-nucleon) effects on CC neutrino-nucleus interactions were studied. In a recent publication by MINER ν A collaboration [41], they studied the uncertainty in the nuclear models using Carbon target by considering events with and without RPA effects and for RPA+2p-2h events and observed that the models require a modification. Further, in more recent results [42], they tuned the 2p-2h model which matched with the previous results [41]. In Ankowski's paper [43], they compare the kinematic and calorimetric methods of energy reconstruction in the disappearance experiments operating in different energy regimes. Some other similar studies can be found in Refs. [44, 45].

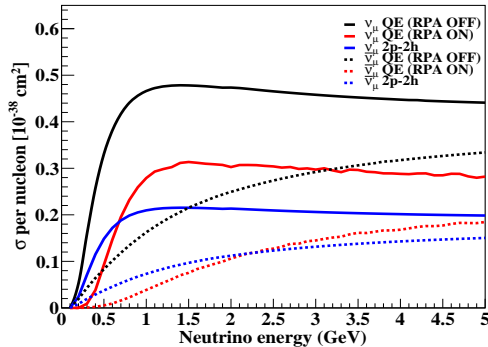


FIG. 2: Cross section for both neutrino (solid line) and anti-neutrino (dotted line) for QE with RPA OFF (black line) and ON (red line), and 2p2h (blue line) interactions.

Keeping the above issues in mind, we have undertaken this work to investigate the effect of many nucleons in the Carbon target at NO ν A experiment on the extraction of neutrino oscillation parameters. We analyse the disappearance channel for NO ν A experiment in this work. First, we compute the neutrino scattering cross-section for various relevant processes, as explained in detail in later sections. Next, we obtain the event spectrum at ND, followed by that at the FD. Events and migration matrices are computed using a stable version (v-2.12.8) of event generator GENIE [46] (Generates Events for Neutrino Interaction Experiments). We have used the kinematic method of energy reconstruction, and Feldman's technique [47] to do the χ^2 analysis. Currently many major neutrino baseline experiments such as MINER ν A [48], MINOS [49], MicroBooNE [50], NO ν A, T2K and LBNE [51] (LBNE is now called DUNE) are using GENIE as event generator. NO ν A uses GENIE (v-2.12.2) [59] tuned to external and NO ν A data for modelling neutrino beam interactions. The detailed procedure to obtain the oscillated event spectrum at FD has been explained in later sections. The unoscillated event spectrum at ND is also used, to take care of the systematics, along with the F/N (Far/Near) ratio of the detectors. Finally, this spectrum of events is used in the sensitivity analysis of extraction of neutrino oscillation parameters. We want to make it clear that we have not attempted to compare NO ν A data with our results - rather, the focus has been to do a simulation to study the effects of multi-nuclear interaction on sensitivity analysis.

The novel feature of this work is that we have studied the individual contribution of 2p-2h and RPA MN interactions along with QE interaction to the neutrino and antineutrino sensitivity analysis and also to FD events. We consider the effect of short range correlations (SRC) also, which NO ν A ignored in their analyses. Detector efficiency and energy resolution are also taken into account, and we found that the oscillation probability curve with 80% detector efficiency is closest to the curve with no detector effects (than the one with 31.2% detector efficiency) - it implies that lower efficiency of the detector causes more uncertainty, as it should be. We would like to mention that no detector effects are equivalent to 100% detector efficiency. To see how RPA and 2p-2h effects influence the event distributions, we have shown the spectrum of QE events with and without RPA corrections in ND, both for neutrino and antineutrino in Fig. 3. The same for FD is shown in Fig. 5 and 6. We find that the 2p-2h and RPA MN interactions affect the cross-section significantly and their effect, in turn, is reflected in event spectrum and extraction of neutrino oscillation parameters alike. They not only suppress the cross-section but also shift the position of the peak in it. These effects increase the area of allowed parameter space in the sensitivity contours of oscillation parameters - which may be understood as an increase in uncertainty.

The paper has been organized as follows - in section II, we briefly review the necessary details of NO ν A experiment, for the completeness of this work. We discuss the multi-nucleon effects (2p-2h, RPA) in section III. Section IV contains the necessary physics and simulation details, where we discuss the numerical method of our analysis, detector effects, the extrapolation technique used to predict the far detector energy spectrum of events, and sensitivity in the extraction of the oscillation parameters. In Section V, we present our results and then discuss them. This analysis is done for both neutrino and antineutrino incoming beams for different processes: QE (without RPA suppression), QE (with RPA suppression), and 2p-2h. We summarize and conclude the work in Section VI.

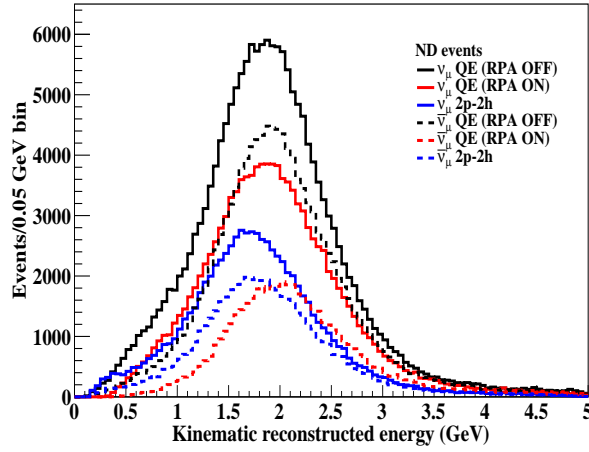


FIG. 3: Events vs. kinematic reconstructed energy of ν_μ for both neutrinos (solid line) and antineutrinos (dotted line). Events are shown for three different interactions: QE without RPA (black line), QE with RPA (red line), and 2p-2h/MEC (blue line).

II. THE NO ν A EXPERIMENT

The NuMI Off-Axis ν_e Appearance or NO ν A is a long-baseline neutrino experiment which consists of two functionally identical, segmented, tracking calorimetric detectors - ND and FD to measure the muon neutrino (ν_μ) disappearance probability $P(\nu_\mu(\bar{\nu}_\mu) \rightarrow \nu_\mu(\bar{\nu}_\mu))$ and electron neutrino (ν_e) appearance probability $P(\nu_\mu \rightarrow \nu_e)$. The $3.8 \text{ m} \times 3.8 \text{ m} \times 12.8 \text{ m}$ ND has a mass of about 0.3 kilotons and is placed 105 m underground, 1 km from Neutrinos at the Main Injector (NuMI) beam at Fermilab [13], USA. The $15 \text{ m} \times 15 \text{ m} \times 60 \text{ m}$ 14 kiloton FD is located near Ash River, Minnesota at a distance of 810 km from the NuMI [53] target. Both the detectors are placed 14.6 mrad off-axis from the center of the NuMI beam to provide a narrow beam neutrino flux peaked at around ~ 2 GeV and to enhance the sensitivity to ν_μ disappearance and ν_e appearance processes. A high-intensity neutrino beam is generated by the collision of 120 GeV protons coming from NuMI onto a 1.2 m graphite target. Pions and kaons produced in the target are focused on by two magnetic horns. In the NuMI beam, most of the neutrinos result from the process $\pi^\pm \rightarrow \mu^\pm + \nu$. The produced neutrino beam contains-95% ν_μ , 4% $\bar{\nu}_\mu$, 1% $\nu_e/\bar{\nu}_e$ (93% $\bar{\nu}_\mu$, 6% ν_μ , 1% $\nu_e/\bar{\nu}_e$ for antineutrino beam). In neutrino experiments, the statistics are measured in terms of protons delivered to the target (POT). Currently, NO ν A has collected 13.6×10^{20} POT with neutrino beam and 12.5×10^{20} POT with antineutrino beam. As the size of the ND is smaller than FD, the ND cannot contain neutrinos having high energy, therefore it observes neutrino spectrum towards lower energy region with smaller hadronic activity and shorter muon tracks. The main objective of these two functionally equivalent detectors placing at a long distance is to measure neutrino oscillation, reduce systematic uncertainty, and from these oscillation measurements NO ν A is expected to determine mass hierarchy, leptonic CP-violating phase δ_{CP} , and also resolve the Octant degeneracy of the atmospheric mixing angle θ_{23} [54–56]. The detectors are made of organic liquid-scintillator and filled with highly reflective white polyvinyl chloride (PVC) of cross-section $3.9 \times 6.6 \text{ cm}^2$ and of length 3.9 m (ND) or 15.5 m (FD). The liquid scintillator consists of 62% of the fiducial mass of each detector.

The primary goal of the ND is to measure the unoscillated neutrino events. It is placed at the same off-axis angle as the FD to maintain the neutrino flux similarity between the two detectors. As the ND is only 1 km from the NuMI, therefore it receives high-intensity neutrino beams than the FD. The cosmic background of ND is almost negligible as it is placed 100 m underground. Because of the off-axis configuration, the neutral current events are suppressed and it helps to increase the purity of ν_μ CC events by simply reducing the charged pions background. The unoscillated flux measured at ND is not the same as the oscillated flux at FD because FD sees neutrino beam as a point source, whereas ND sees neutrino beam as broadband.

III. MULTI-NUCLEON INTERACTIONS

Currently, the neutrino scattering community is more interested in a process beyond QE and resonance processes, when neutrino scatters off a nucleus. In this process, when a neutrino interacts with the nucleons inside the nucleus exchanging a W boson, it is absorbed by nucleons which results in the knock out of two-particle and two-hole pairs (2p-2h) through an exchange of a meson. QE interaction is referred to as 1p-1h interactions because one particle is ejected out from the nucleus leaving one empty unoccupied (hole) energy state. Together multi-nucleon excitation and charged lepton in the final state (without pion absorption) are known as quasielastic (QE)-like events. 2p-2h events mostly occur in the energy region between QE and resonance production. This process contributes significantly to the neutrino-nucleus scattering and its contribution can be observed in the cross-section plot in Fig. 2. There are several major processes which result in two (or more) nucleons and a excited spectator nucleus with two (or more) holes-nucleon correlations in the initial state, neutrino coupling to 2p-2h, and FSI. The nucleon-nucleon correlations in the initial state are often known as short range correlations [30]. In QE interactions, the Relativistic Fermi Gas model (RFG) is used to describe the nuclear effects, which is based on a simple independent particle model known as the Fermi Gas model. The RFG model has been modified by A. Bodek and J.L Ritchie [31] to incorporate short range nucleon-nucleon correlations. In this model, all nucleons inside the nucleus are uncorrelated. If we consider that the nucleons are correlated and two nucleons are separated by a distance < 15 fm then short range correlations involved. These short-range strong forces increase their relative momentum more than Fermi momenta which results ejection of two nucleons. As two nucleons are knocked out from the target nucleus, the momentum distribution of the remaining nucleon system is affected. Some works on np-nh contribution to neutrino-nucleus cross-section can be found in - (phenomenological approaches) by Mosel et. al. [32, 33, 57], Bodek et. al. [58]. In GENIE two models are available for MEC process and $\text{NO}\nu\text{A}$ uses both the Empirical and Valencia MEC models [59]. It is clear from their analysis that any MEC model present in GENIE requires significant tuning to reproduce their data. We choose the Empirical MEC model for our analysis as it is the only model available in GENIE which includes a neutral-current component.

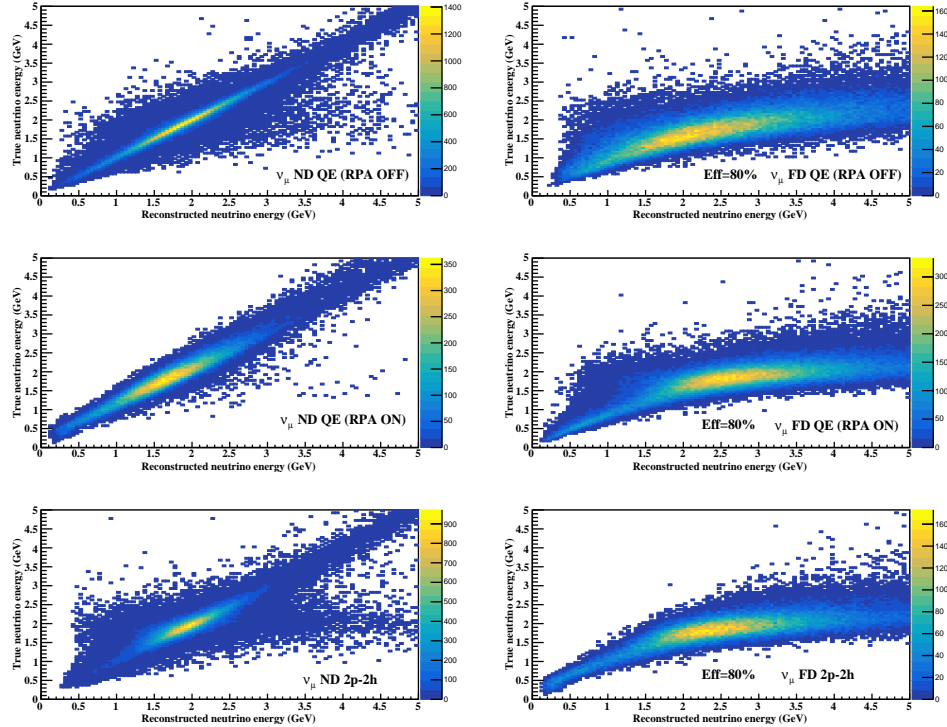


FIG. 4: Reco-to-true and true-to-reco migration matrices for ND (left) and FD (right) events for three different interactions with FD detector efficiency 80%. For each detector a 2D histogram of reconstructed energy vs. true energy is created. Using these reco-true matrices, ND neutrino spectrums in bins of reconstructed energy are converted to bins of true energy and vice versa for FD energy spectrum.

IV. PHYSICS AND SIMULATION DETAILS OF THIS WORK

For investigating the effect of multi-nucleon interactions on measurement sensitivity of neutrino oscillation parameters, as stated earlier, in this work we consider charged current (CC) QE, RES, DIS, and 2p-2h interactions. We have generated 1 million MC events for both ND and FD using NO ν A flux in the energy range 0.0-5.0 GeV to measure the energy spectrum of ν_μ ($\bar{\nu}_\mu$) CC interactions in both detectors, and calculated reconstruction energy using kinematic method (equation (2)). We have used GENIE default models for simulation- QE scattering predicted according to Llewellyn-Smith [60], resonance (RES) processes according to Rein-Sehgal model [23] with 16 resonance models while DIS interactions formulated by Bodek and Yang model [61]. For modelling 2p-2h interaction, we have used empirical model [62]. Furthermore, we have tuned GENIE's description to include long range nucleon correlations - the RPA effect with the Nieves model and to include short range correlations we use RFG model. The electromagnetic form factor can be parameterized by vector form factor BBBA2005 model [63] with a variable value of axial mass M_A between 0.99-1.2 GeV/ c^2 . We have used default axial mass $M_A=0.99$ GeV/ c^2 . FSI are modelled with the INTRANUKE [64] cascade model. RFG is currently used as the main model in the analysis of long-baseline experiments to get high-precision measurements of the neutrino oscillation parameters. Inside the nucleus, the motion of the nucleons can be understood in two different ways - GENIE and Nieves. In GENIE, global Fermi Gas (GFG) is used to model the nucleus, where the nucleus is assumed to have constant nuclear density and with a uniform momentum distribution in 3-D momentum space. On the other hand, the Nieves model considers the nucleus as a

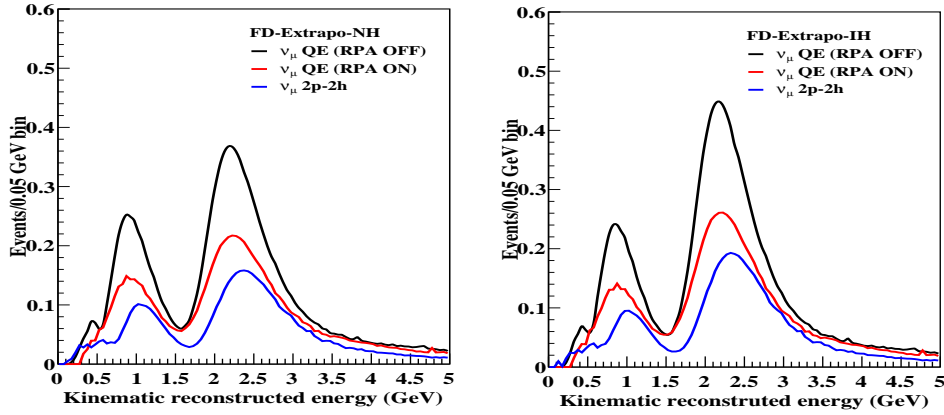


FIG. 5: Left and right panel shows extrapolated FD events as a function of reconstructed ν_μ energy for both NH and IH. Events are shown for three different interactions: QE without RPA (black line), QE with RPA (red line), and 2p-2h (blue line).

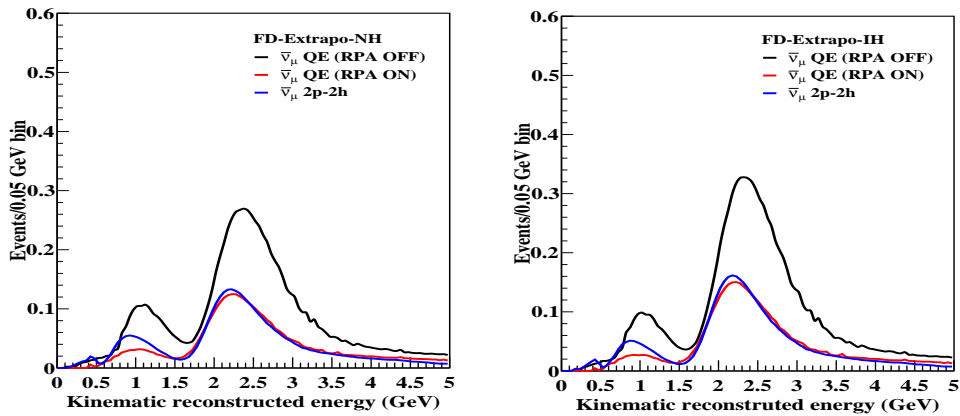


FIG. 6: Left and right panel shows extrapolated FD events as a function of reconstructed $\bar{\nu}_\mu$ energy for both NH and IH. Events are shown for three different interactions: QE without RPA (black line), QE with RPA (red line), and 2p-2h (blue line).

local Fermi Gas (LFG) which is a minimal extension of the RFG model. In the LFG model, the Fermi momentum and binding energy depend on the distance, i.e., the radial position of the nucleons in the nucleus. NO ν A uses models developed by Valencia group for QE and 2p-2h [65] interactions, and neglect the influence of short range correlations as they have used LFG model to describe the initial nuclear state in both Valencia QE and 2p-2h models. They have simulated RES processes using Berger-Sehgal model and DIS by Bodek-Yang model [66].

A. Oscillation Analysis

In the neutrino oscillation analysis, the significant background contribution comes from neutral current events which are wrongly identified as CC events. The cosmic background contributes 4.1% of the selected FD ν_μ CC events and NC background events contributes 6% of FD ν_μ CC events [67]. In general, this contribution is considered to be very low, therefore in our analysis, we have neglected it. The relevant oscillation probability for NO ν A for the disappearance channel can be expressed as [68]

$$P(\nu_\mu \rightarrow \nu_\mu) = 1 - \sin^2 2\theta_{23} \sin^2 \Delta_{32} + 4 \sin^2 \theta_{23} \sin^2 \theta_{13} \cos^2 2\theta_{23} \sin^2 \Delta_{32} \quad (1)$$

where $\Delta_{ij} = \frac{\Delta m_{ij}^2 L}{4E_\nu}$, Δm_{ij}^2 are the mass differences and θ_{ij} are the mixing angles. The true (global best fit) values of the oscillation parameters used in the work are shown in Table I.

parameter	best fit	3σ range
$\Delta m_{21}^2 [10^{-5} eV^2]$	7.50	6.94 – 8.14
$ \Delta m_{31}^2 [10^{-3} eV^2] (\text{NH})$	2.56	2.46 – 2.65
$ \Delta m_{31}^2 [10^{-3} eV^2] (\text{IH})$	2.46	2.37 – 2.55
$\sin^2 \theta_{23} / 10^{-1} (\text{NH})$	5.66	4.46 – 6.09
$\sin^2 \theta_{23} / 10^{-1} (\text{IH})$	5.66	4.41 – 6.09
$\sin^2 \theta_{13} / 10^{-1} (\text{NH})$	2.225	2.015 – 2.417
$\sin^2 \theta_{13} / 10^{-1} (\text{IH})$	2.250	2.039 – 2.441

TABLE I: 3σ values of neutrino oscillation parameters taken from [69].

B. Energy Reconstruction

The neutrino energy is constructed using kinematic reconstruction method which relies on the kinematics of outgoing lepton l (energy and angle). This method of neutrino energy reconstruction is based on the assumptions that the beam particle interacts with a single neutron at rest with constant binding energy and that no other nucleons are knocked out from the nucleus. For a QE event, the neutrino energy can be reconstructed as [36]:

$$E_\nu^{QE} = \frac{2(M_n - E_b)E_l - (E_b^2 - 2M_n E_b + \Delta M^2)}{2(M_n - E_b - E_l + p_l \cos \theta_l)} \quad (2)$$

where $\Delta M^2 = M_n^2 - M_p^2 + m_l^2$ and E_b is the average binding energy of the neutron inside the nucleus. M_n is the free neutron rest mass, E_l and θ_l are the energy and angle of the outgoing lepton respectively. This equation is exact only for QE interaction with the neutron at rest.

C. Extrapolation Technique

After selecting the ND events, the next step is to predict the corresponding number of interactions in the FD. The technique of predicting the FD energy spectrum using ND data is known as extrapolation. NO ν A uses Monte Carlo simulation to extrapolate the neutrino energy spectrum measured in the ND to the FD. Monte Carlo simulations for ND and FD are generated separately under the assumption of no neutrino oscillation. The ν_μ ($\bar{\nu}_\mu$) signal spectra at the FD are predicted for both neutrino and antineutrino beams separately based on the constrained ν_μ ($\bar{\nu}_\mu$) event predictions in the ND. The discrepancy between ND and FD spectra mainly is due to the geometric effects. Using this technique, the smearing effect of imperfect energy resolution in both the detectors can be detected. This is done

by creating a 2D histogram between the reconstructed energy and true energy in ND and FD detectors. Further, these histograms are used to re-weight the reconstruct and true spectrum to get the extrapolated FD events. The extrapolation of ν_μ ($\bar{\nu}_\mu$) CC signal is done in bins of true energy. The full procedure of extrapolation can be explained as follows [16, 18, 70, 71]:

1. The reconstructed ND energy spectrum (X-axis) is converted to the spectrum in bins of true of energy (Y-axis) with the help of reco-to-true migration matrix from simulation. Each element of the matrix represents the probability that a neutrino with reconstructed energy E_i came from a neutrino with true energy E_j where j is the index over true energy, i.e., for each given value of the reconstructed energy, a probability distribution in true energies can be computed. As the number of events before and after migration should remain the same, it is required that sum of probability densities for a given true energy to be normalized to the unity. The migration matrices used for three different processes in ND and FD are illustrated in Fig. 4.
2. The geometric effect (e.g., angular acceptance, decay kinematics, beamline geometry, focusing of the particles) is taken care of by multiplying this true energy spectrum with a far-to-near ratio to get FD unoscillated prediction in bins of true energy. The main advantage of this approach is the reduction of many systematic uncertainties that affect both detectors, resulting in a smaller error on the oscillation measurements. This ratio also includes the efficiency and acceptance differences between the two detectors, differences in detector fiducial volumes, and differences in the flux at the ND and FD [70].
3. Then this true energy spectrum is multiplied with oscillation probability to re-weight the spectrum.
4. Finally, using underlying energy distributions from simulated neutrino interactions in the FD (true-to-reco migration matrix) this oscillated spectrum in bins of true energy is mapped to the spectrum in bins of reconstructed energy.

The extrapolated FD energy spectrum predicted from the simulated ND energy spectrum is shown in Figs. 5 and 6 for both neutrino and anti-neutrino and both the mass hierarchies.

D. Detector Effect

The neutrino energy resolution at NO ν A experiment at the FD is 9.1% (8.1%) for ν_μ CC ($\bar{\nu}_\mu$ CC) events. The efficiency of selection of ν_μ ($\bar{\nu}_\mu$) events is 31.2% (33.9%) relative to true interactions in the fiducial volume which results in 98.6% (98.8%) purity at the FD during neutrino (anti-neutrino) beam [13]. For the disappearance channel, both ν_μ and $\bar{\nu}_\mu$ are considered as the signal. We have considered detector efficiency 31.2% (ν_μ) and 33.9% ($\bar{\nu}_\mu$) for sensitivity analysis and also compare it with the other two values for comparison - just to see what happens if the detector performance is improved by 50% or 80%.

E. Sensitivity analysis of neutrino oscillation parameters

Next, we focus on the sensitivity study of the neutrino oscillation parameters θ_{23} and Δm_{32}^2 , applying the result of the above-discussed analysis of multi-nucleon effects (as the ν_μ disappearance channel is sensitive to $\sin^2 \theta_{23}$ and $|\Delta m_{32}^2|$). This would bring us closer to the aim of this investigation - how the multi-nucleon interactions in the target nucleus affect the measurement of neutrino oscillation parameters at NO ν A experiment. The allowed confidence level regions in parameter spaces are obtained using the Feldman-Cousins method [47]. We calculate the acceptance region of each point in the $\sin^2 \theta_{23}$ - Δm_{32}^2 plane by performing a Monte Carlo simulation of the results obtained from a large number of simulated experiments for the given set of unknown physical parameters with the known neutrino flux of the actual experiment using,

$$\Delta\chi^2 = 2 \sum_i \left[\mu_i - \mu_{best_i} + \mu_{best_i} \ln \left(\frac{\mu_{best_i} + b_i}{\mu_i + b_i} \right) \right] \quad (3)$$

where the sums runs over all bins, b_i is the mean expected background, μ_i is the number of predicted events for i^{th} bin, and μ_{best_i} is the number of observed events for i^{th} bin in FD data. The predicted μ_i depends on the values chosen for θ_{13} , θ_{23} , Δm_{32}^2 , Δm_{21}^2 . We have neglected the background contribution. We determine the value of $\Delta\chi^2$ for each simulated experiment and $\Delta\chi_c^2(\sin^2 \theta_{23}, \Delta m^2)$ is the critical value corresponding to desired precision. After

the data analysis, comparing $\Delta\chi^2(N|\sin^2\theta_{23}, \Delta m_{32}^2)$ with $\Delta\chi_c^2$, the acceptance region for all point is obtained by imposing the condition

$$\Delta\chi^2(N|\sin^2\theta_{23}, \Delta m_{32}^2) < \Delta\chi_c^2(\sin^2\theta_{23}, \Delta m_{32}^2) \quad (4)$$

The log-likelihood function is calculated for different oscillation parameters and 2D surface of χ^2 vs Δm_{32}^2 and $\sin^2\theta_{23}$ is formed. The values of $\Delta\chi^2$ for different σ and confidence intervals in 2D case is shown in Table 2.

Sigma	CL (%)	2D
1 σ	68.3	2.30
2 σ	95.45	6.18
3 σ	99.73	11.83

TABLE II: $\Delta\chi^2$ for two dimensions for different σ and confidence levels.

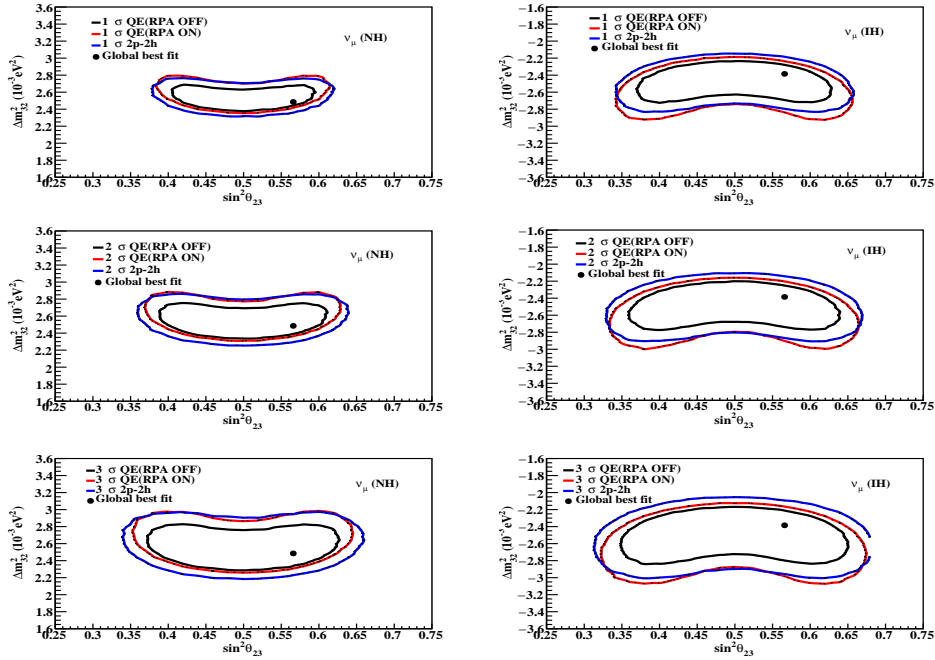


FIG. 7: Comparison of 1 σ , 2 σ and 3 σ contours for Δm_{32}^2 vs $\sin^2\theta_{23}$ for three different interactions QE without RPA (black solid line), QE with RPA suppression (red solid line) and 2p-2h (blue solid line) for NH (left panel) and IH (right panel) for neutrino without detector response. The global best-fit point is shown by a black marker.

V. RESULTS AND DISCUSSION

In this section, we present the results on sensitivity analysis of the ν_μ and $\bar{\nu}_\mu$ disappearance channel at NO ν A, and also a discussion on them. The extrapolated neutrino and antineutrino FD events prediction are computed in a three neutrino flavor oscillation model where the ν and $\bar{\nu}$ parameters-atmospheric mass splitting Δm_{32}^2 and θ_{23} mixing angles are allowed to vary independently. The results are presented in Fig. 2 and Figs. (3-14). The ND flux used is shown in Fig. 1. In Fig. 2, we have shown how the MN interactions (RPA and 2p-2h) affect the neutrino-nucleon cross-section for the Carbon target (per nucleon). We have plotted QE interactions without RPA effects (black line), with RPA effects (red line) and 2p-2h interactions (blue line) for neutrinos (solid lines) and anti-neutrinos (dotted lines). The ND events spectrum for neutrino and antineutrino is shown in Fig. 3. Migration matrices generated and then used for ND and FD are shown in Fig. 4. The extrapolated event distribution as a function of reconstructed energy at FD is shown in Fig. 5 (neutrino) and Fig. 6 (antineutrino). The results of sensitivity analysis are presented in Figs. (7-14). We compare sensitivity results separately for 1 σ , 2 σ , and 3 σ contours for QE without RPA, with

RPA and 2p-2h interactions for NH (left panel) and IH (right panel) for neutrino in Fig. 7, and anti-neutrino in Fig. 8, without detector effect to observe the differences due to MN interactions. In Figs. 9, detector effects have been included, but RPA effects not included, while in Fig 10, both detector and RPA effects have been included. Results with including detector and 2p-2h effects have been shown in Fig 11. Fig (9-11) is for neutrino, while Fig. (12-14) is same but for antineutrino.

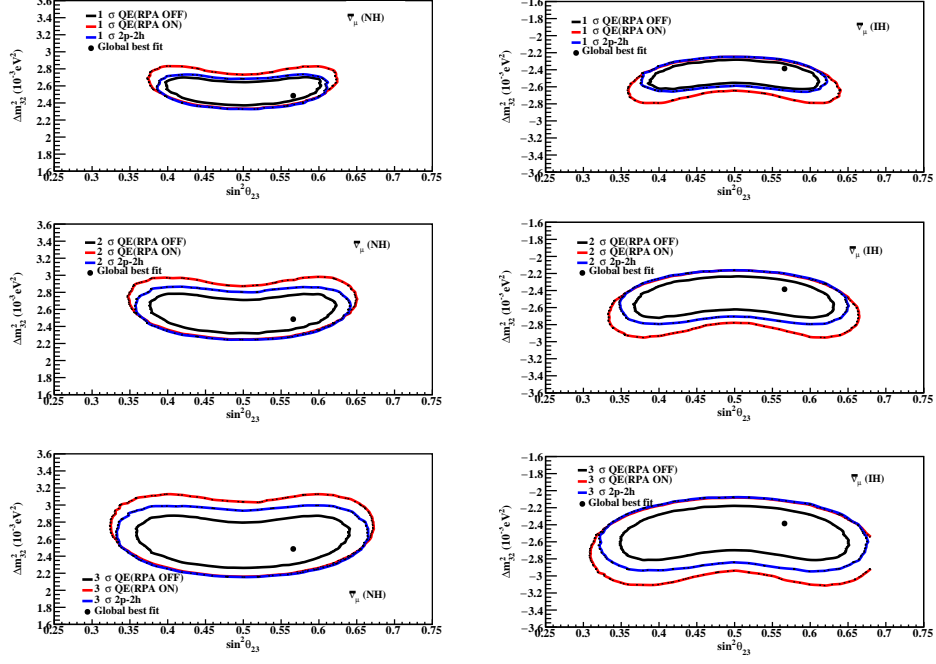


FIG. 8: Comparison of 1σ , 2σ and 3σ contours for Δm_{32}^2 vs $\sin^2 \theta_{23}$ for antineutrino without detector response.

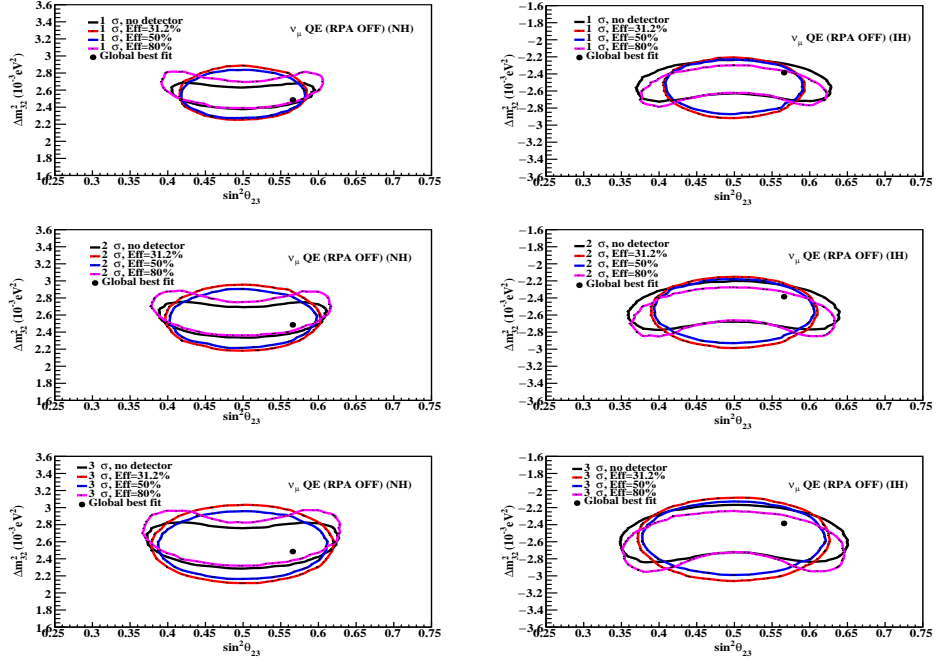


FIG. 9: Comparison of 1 σ , 2 σ and 3 σ contours in Δm^2_{32} vs $\sin^2 \theta_{23}$ for QE without RPA for NH (left panel) and IH (right panel) for neutrino mode with/without detector effect. Here black solid line represents the no detector effect, red solid line detector effect with 31.2% efficiency, blue solid line 50% efficiency and magenta solid line 80% efficiency.

In all these Figs. (7-11), left panel is for NH, while right panel is for IH. Figs. (7-11) are shown with no detector effect (black line), detector effect with efficiency 31.2% (ν_μ) or 33.9% ($\bar{\nu}_\mu$) (red line), 50% (blue line) and 80% (magenta line) for comparison.

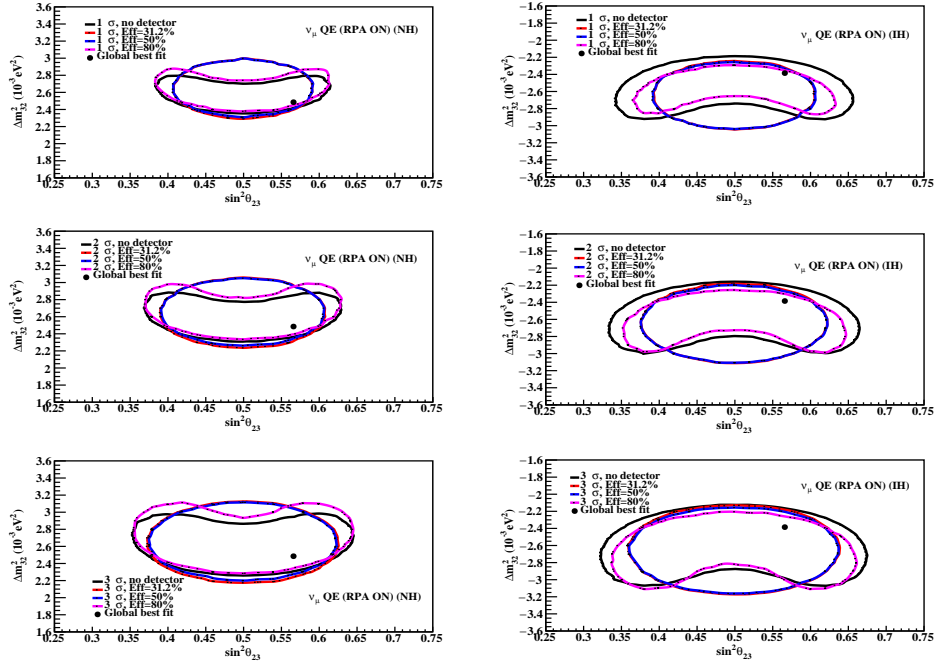


FIG. 10: Same as in Fig. 9, but for QE with RPA.

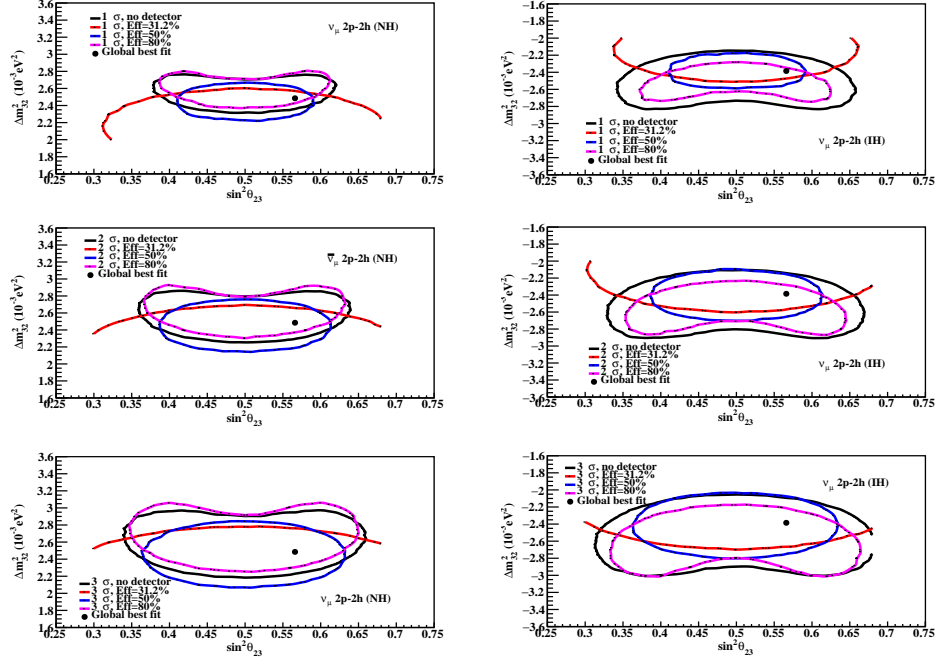
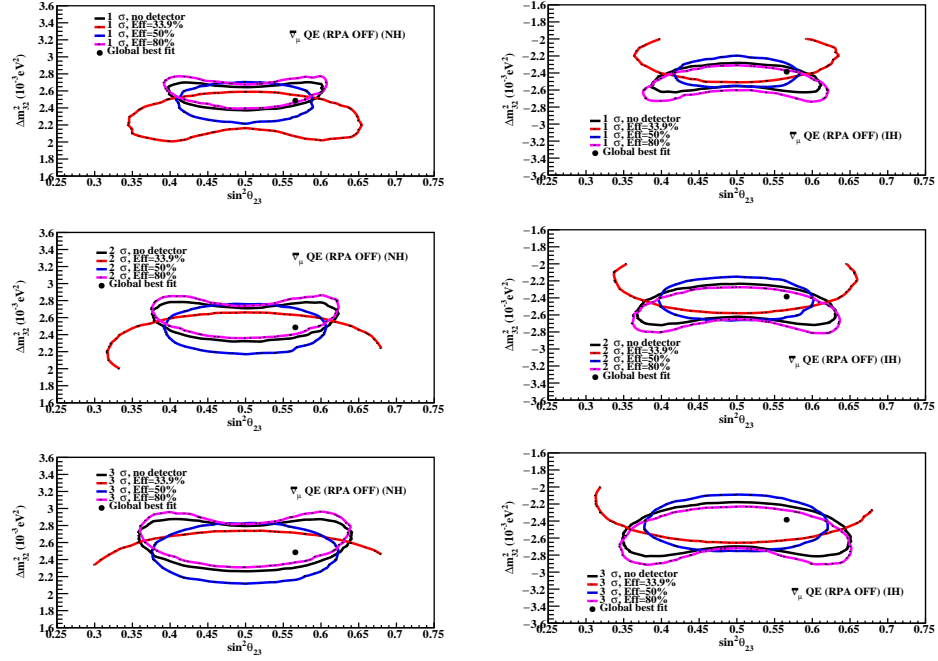


FIG. 11: Same as in Fig. 9, but for 2p-2h.

FIG. 12: Comparison of 1 σ , 2 σ and 3 σ contours in Δm^2_{32} vs $\sin^2 \theta_{23}$ for QE without RPA for NH (left panel) and IH (right panel) for anti-neutrino mode with/without detector effect. Here black solid line represents the no detector effect, red solid line detector effect with 33.9% efficiency, blue solid line 50% efficiency and magenta solid line 80% efficiency.

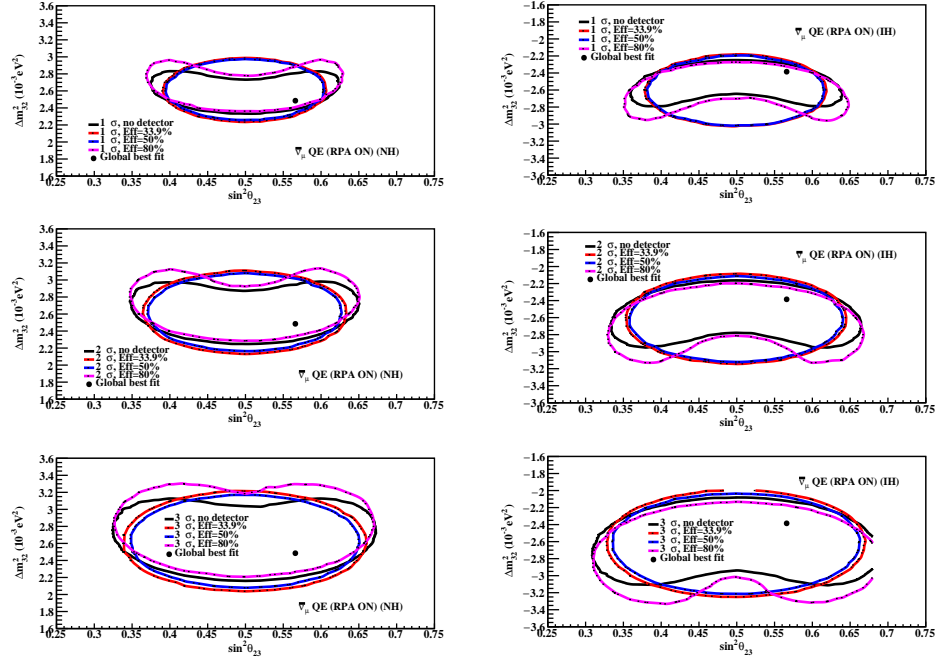


FIG. 13: Same as in Fig. 12, but for QE with RPA.

From Fig. 2, it is evident that MN interactions not only suppress the cross-section but shift the position of the peak in the cross-section too. As a result of which, a similar feature is observed in Fig. 3 for the event spectrum at the ND. From the left panel of Fig. 3, we observe that suppression due to 2p-2h is more than that of RPA, and in the 2p-2h case, the position of peak shifts to slightly lower neutrino energy. However, suppression for antineutrino is found to be similar for both RPA and 2p-2h, and in 2p-2h, the position of peak shifts to slightly lower energy, while for RPA it shifts to slightly higher energy. From the corresponding spectrum of events at FD, after using the extrapolation technique, in Fig. 5, the oscillatory nature of neutrino oscillation probability can be seen. It may be noted that the results shown in Figs. 5 and 6 are the outcomes of folding of flux (Fig. 1), cross-section (Fig. 2), ND events spectrum (Fig. 3), and oscillation probability (calculated using equation (1)) as we know neutrino event rates are a convolution of neutrino flux, neutrino-nucleon cross-section, nuclear effects, and detector response. Both for neutrino and antineutrino, there is a clear distinction among the three curves - pure CC QE, QE with RPA and 2p-2h interactions, in medium energy ranges, say $0.5 \leq E_\nu \leq 3$ GeV and $0.5 \leq E_{\bar{\nu}} \leq 4.5$ GeV respectively. It implies that at energies beyond these ranges, the effect of these interactions diminish. These observations can be attributed to the fundamental structure and nature of these interactions in these energy ranges as also discussed in the introduction. Also, from Figs. 5 and 6, we find that as the MN effects decrease the separation between two peaks of FD events spectrum, it is expected to increase the uncertainty in the measurement of oscillation parameters - as we know that amplitude and phase in oscillation probability are reflected in measurement in the experiments. Next, we would like to present a discussion on the results of sensitivity analysis shown in Figs. (7-14), which can be summarised as follows:

1. From Figs. 7 and 8, we observe that including MN effects increase the area of the sensitivity contour, and hence can say that the uncertainty increases.
2. Also from Figs. 7 and 8, we can say that the areas enclosed by the contours without detector effect, before and after including MN effects are more in antineutrino than neutrino - which again can be attributed to less flux and cross-section for antineutrino (please see Fig. 1. and 2. respectively). And, there is more separation between contours of with and without MN interactions (reflection of Fig. 5 and 6), as compared to that of neutrino case. So, we can say that MN interactions affect antineutrino scattering more than that of neutrino.
3. Similarly, from Figs. 9-14, it is observed that the sensitivity contours with 80% detector efficiency are the closest to those with no detector effect (which indeed corresponds to 100% detector efficiency and no inclusion of the resolution function for detector). The lower the efficiency of the detector, the more is the allowed region of parameter space, and hence more uncertainty.

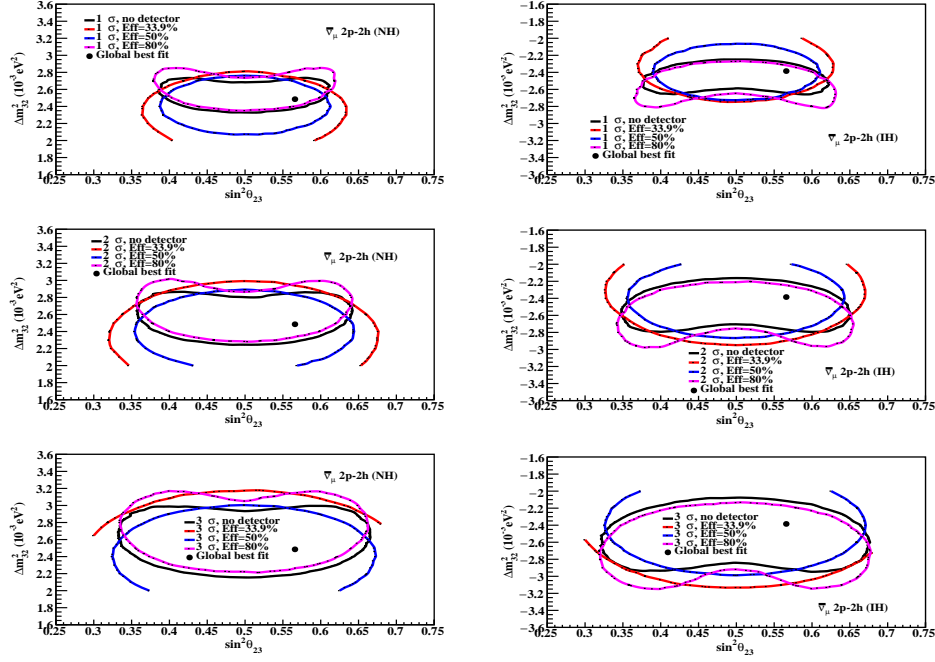


FIG. 14: Same as in Fig. 12, but for 2p-2h.

VI. SUMMARY AND CONCLUSION

To summarise, in this work, we studied the effect of MN interactions at NO ν A experiment (Carbon target), using disappearance channel, on the sensitivity of measurement of atmospheric mixing angle θ_{23} and Δm_{32}^2 . In particular, we considered RPA and 2p-2h interactions. We used event generator GENIE for the purpose, along with extrapolation technique for computing FD events spectrum and Feldman's technique for the χ^2 analysis. In their latest analysis [66], NO ν A uses only Nieves model for QE scattering, while we have considered both Llewellyn-Smith and Nieves model and shown the event distribution and sensitivity analysis using both the two models. To include short-range nucleon-nucleon correlations, RFG model is taken as the nuclear model whereas in NO ν A the initial nuclear state in both Valencia QE and 2p-2h models are represented by local Fermi gas which does not consider short-range correlations. For 2p-2h modelling, we consider the Empirical model and NO ν A considered Valencia (Nieves et. al.) model. Migration matrices were generated and used both for both ND and FD. We did the analysis with/without detector effects, and for both the hierarchies (NH and IH). The global best fit central values from [69] were used as a true set for the χ^2 analysis, while their 3σ range was used for simulated experiments (test values). We used the kinematical method of energy reconstruction, and 1 million MC events were generated for simulation at ND and FD. We found that the MN interactions not only suppress the cross-section but shift the position of the peak in the cross-section too. As a result of which, a similar feature is observed for the event spectrum at the ND, and suppression due to 2p-2h is more than that of RPA, and in the 2p-2h case, the position of peak shifts to slightly lower neutrino energy. However, suppression for antineutrino is found to be similar for both RPA and 2p-2h, and in 2p-2h, the position of peak shifts to slightly lower energy, while for RPA it shifts to slightly higher energy. From the corresponding spectrum of events at FD, the oscillatory nature of neutrino oscillation probability can be seen, after using the extrapolation technique. Both for neutrino and antineutrino, there is clear distinction among the three curves - pure CCQE, QE with RPA and 2p-2h interactions, in medium energy ranges, say $0.5 \leq E_\nu \leq 3$ GeV and $0.5 \leq E_\nu \leq 4.5$ GeV respectively. This may be an indication that at energies beyond these ranges, the effect of these interactions diminish and hence all the three curve tend to merge.

It was observed that as the MN effects decrease the separation between two peaks of FD events spectrum, it increased the uncertainty in the measurement of oscillation parameters (since the amplitude and phase in oscillation probability are reflected in measurement in the experiments). The areas before and after including MN effects are more in antineutrino than neutrino - which again can be attributed to less flux and cross-section for antineutrino (and hence more uncertainty due to less data). For antineutrino, there was more separation between contours of

with and without MN interactions, as compared to that of neutrino case. So, we can say that MN interactions affect antineutrino more than a neutrino. Results were presented for both hierarchies, and respective changes are seen in both of them. The sensitivity contours with 80% efficiency were found to be the closest to those with no detector effect (which corresponds to 100% detector efficiency). The lower efficiency of the detector implies more uncertainty in sensitivity studies.

To conclude, multi-nucleon interactions (2p-2h and RPA discussed here) along with effect of short range correlations, increase the uncertainty in the measurement of neutrino oscillation parameters, and hence command a more careful inclusion of them in sensitivity measurements analysis. Better detector efficiency is reflected in more precise results. The results presented here can give useful insight into precision studies at long baseline neutrino experiments in future measurements - specially on the precision measurement of CPV phase δ_{CP} and Octant of θ_{23} . The calorimetric method of neutrino energy reconstruction may provide more precise results and in the future, we aim to use it for a better understanding of the systematic uncertainties due to multi-nucleon effects. This study will help to improve the existing models in event generators to reduce the impact of systematic uncertainties, which in turn may prove to be beneficial for all current ongoing and future experiments such as NO ν A and DUNE.

VII. ACKNOWLEDGMENT

KB thanks DST-SERB, Govt. of India, for support through her major project EMR/2014/000296, during which a part of this work was done. She also would like to acknowledge some support from Gauhati University in her laboratory. KB, NS and JS thank Prof. Raj Gandhi of HRI, Prayagraj for discussions during the initial stages of the work.

VIII. REFERENCES

-
- [1] Y. Fukuda *et al.* [Super-Kamiokande], Phys. Rev. Lett. **81**, 1562-1567 (1998) doi:10.1103/PhysRevLett.81.1562 [arXiv:hep-ex/9807003 [hep-ex]].
 - [2] S. Fukuda *et al.* [Super-Kamiokande], Phys. Lett. B **539**, 179-187 (2002) doi:10.1016/S0370-2693(02)02090-7 [arXiv:hep-ex/0205075 [hep-ex]].
 - [3] Q. R. Ahmad *et al.* [SNO], Phys. Rev. Lett. **89**, 011301 (2002) doi:10.1103/PhysRevLett.89.011301 [arXiv:nucl-ex/0204008 [nucl-ex]].
 - [4] K. Eguchi *et al.* [KamLAND], Phys. Rev. Lett. **90**, 021802 (2003) doi:10.1103/PhysRevLett.90.021802 [arXiv:hep-ex/0212021 [hep-ex]].
 - [5] D. G. Michael *et al.* [MINOS], Phys. Rev. Lett. **97**, 191801 (2006) doi:10.1103/PhysRevLett.97.191801 [arXiv:hep-ex/0607088 [hep-ex]].
 - [6] Y. Abe *et al.* [Double Chooz], Phys. Rev. Lett. **108**, 131801 (2012) doi:10.1103/PhysRevLett.108.131801 [arXiv:1112.6353 [hep-ex]].
 - [7] F. P. An *et al.* [Daya Bay], Phys. Rev. Lett. **108**, 171803 (2012) doi:10.1103/PhysRevLett.108.171803 [arXiv:1203.1669 [hep-ex]].
 - [8] J. K. Ahn *et al.* [RENO], Phys. Rev. Lett. **108**, 191802 (2012) doi:10.1103/PhysRevLett.108.191802 [arXiv:1204.0626 [hep-ex]].
 - [9] K. Abe *et al.* [T2K], Phys. Rev. D **96**, no.9, 092006 (2017) [erratum: Phys. Rev. D **98**, no.1, 019902 (2018)] doi:10.1103/PhysRevD.96.092006 [arXiv:1707.01048 [hep-ex]].
 - [10] B. Abi *et al.* [DUNE], JINST **15**, no.08, T08010 (2020) doi:10.1088/1748-0221/15/08/T08010 [arXiv:2002.03010 [physics.ins-det]].
 - [11] D. S. Ayres *et al.* [NO ν A], [arXiv:hep-ex/0503053 [hep-ex]].
 - [12] K. Abe *et al.* [T2K], Phys. Rev. Lett. **121**, no.17, 171802 (2018) doi:10.1103/PhysRevLett.121.171802 [arXiv:1807.07891 [hep-ex]].
 - [13] M. A. Acero *et al.* [NO ν A], Phys. Rev. Lett. **123**, no.15, 151803 (2019) doi:10.1103/PhysRevLett.123.151803 [arXiv:1906.04907 [hep-ex]].
 - [14] K. Abe *et al.* [T2K], Nature **580**, no.7803, 339-344 (2020) [erratum: Nature **583**, no.7814, E16 (2020)] doi:10.1038/s41586-020-2177-0 [arXiv:1910.03887 [hep-ex]].
 - [15] L. S. Miranda, P. Pasquini, U. Rahaman and S. Razzaque, Eur. Phys. J. C **81**, no.5, 444 (2021) doi:10.1140/epjc/s10052-021-09227-0 [arXiv:1911.09398 [hep-ph]].

- [16] P. Adamson *et al.* [NOvA], Phys. Rev. D **93**, no.5, 051104 (2016) doi:10.1103/PhysRevD.93.051104 [arXiv:1601.05037 [hep-ex]].
- [17] P. Adamson *et al.* [NOvA], Phys. Rev. Lett. **116**, no.15, 151806 (2016) doi:10.1103/PhysRevLett.116.151806 [arXiv:1601.05022 [hep-ex]].
- [18] P. Adamson *et al.* [NOvA], Phys. Rev. Lett. **118**, no.15, 151802 (2017) doi:10.1103/PhysRevLett.118.151802 [arXiv:1701.05891 [hep-ex]].
- [19] P. Adamson *et al.* [NOvA], Phys. Rev. Lett. **118**, no.23, 231801 (2017) doi:10.1103/PhysRevLett.118.231801 [arXiv:1703.03328 [hep-ex]].
- [20] M. A. Acero *et al.* [NOvA], Phys. Rev. D **98**, 032012 (2018) doi:10.1103/PhysRevD.98.032012 [arXiv:1806.00096 [hep-ex]].
- [21] D. S. Ayres *et al.* [NOvA], doi:10.2172/935497.
- [22] J. A. Formaggio and G. P. Zeller, Rev. Mod. Phys. **84**, 1307-1341 (2012) doi:10.1103/RevModPhys.84.1307 [arXiv:1305.7513 [hep-ex]].
- [23] D. Rein and L. M. Sehgal, Annals Phys. **133**, 79-153 (1981) doi:10.1016/0003-4916(81)90242-6.
- [24] M. Martini, M. Ericson, G. Chanfray and J. Marteau, Phys. Rev. C **80**, 065501 (2009) doi:10.1103/PhysRevC.80.065501 [arXiv:0910.2622 [nucl-th]].
- [25] M. Martini, M. Ericson, G. Chanfray and J. Marteau, Phys. Rev. C **81**, 045502 (2010) doi:10.1103/PhysRevC.81.045502 [arXiv:1002.4538 [hep-ph]].
- [26] M. Martini, M. Ericson and G. Chanfray, Phys. Rev. C **84**, 055502 (2011) doi:10.1103/PhysRevC.84.055502 [arXiv:1110.0221 [nucl-th]].
- [27] M. Martini, M. Ericson and G. Chanfray, Phys. Rev. D **87**, no.1, 013009 (2013) doi:10.1103/PhysRevD.87.013009 [arXiv:1211.1523 [hep-ph]].
- [28] M. Martini, M. Ericson and G. Chanfray, Phys. Rev. D **85**, 093012 (2012) doi:10.1103/PhysRevD.85.093012 [arXiv:1202.4745 [hep-ph]].
- [29] O. Benhar and N. Rocco, Adv. High Energy Phys. **2013**, 912702 (2013) doi:10.1155/2013/912702 [arXiv:1310.3869 [nucl-th]].
- [30] H. Gallagher, G. Garvey and G. P. Zeller, Ann. Rev. Nucl. Part. Sci. **61**, 355-378 (2011) doi:10.1146/annurev-nucl-102010-130255
- [31] A. Bodek and J. L. Ritchie, Phys. Rev. D **24**, 1400 (1981) doi:10.1103/PhysRevD.24.1400.
- [32] O. Lalakulich, K. Gallmeister and U. Mosel, Phys. Rev. C **86**, no.1, 014614 (2012) [erratum: Phys. Rev. C **90**, no.2, 029902 (2014)] doi:10.1103/PhysRevC.86.014614 [arXiv:1203.2935 [nucl-th]].
- [33] O. Lalakulich, U. Mosel and K. Gallmeister, Phys. Rev. C **86**, 054606 (2012) doi:10.1103/PhysRevC.86.054606 [arXiv:1208.3678 [nucl-th]].
- [34] D. Meloni and M. Martini, Phys. Lett. B **716**, 186-192 (2012) doi:10.1016/j.physletb.2012.08.007 [arXiv:1203.3335 [hep-ph]].
- [35] P. Coloma and P. Huber, Phys. Rev. Lett. **111**, no.22, 221802 (2013) doi:10.1103/PhysRevLett.111.221802 [arXiv:1307.1243 [hep-ph]].
- [36] P. Coloma, P. Huber, C. M. Jen and C. Mariani, Phys. Rev. D **89**, no.7, 073015 (2014) doi:10.1103/PhysRevD.89.073015 [arXiv:1311.4506 [hep-ph]].
- [37] J. Nieves, J. E. Amaro and M. Valverde, Phys. Rev. C **70**, 055503 (2004) [erratum: Phys. Rev. C **72**, 019902 (2005)] doi:10.1103/PhysRevC.70.055503 [arXiv:nucl-th/0408005 [nucl-th]].
- [38] W. M. Alberico, A. Molinari, A. De Pace, M. Ericson and M. B. Johnson, Phys. Rev. C **34**, 977-990 (1986) doi:10.1103/PhysRevC.34.977.
- [39] H. c. Kim, J. Piekarewicz and C. J. Horowitz, Phys. Rev. C **51**, 2739-2749 (1995) doi:10.1103/PhysRevC.51.2739 [arXiv:nucl-th/9412017 [nucl-th]].
- [40] J. Nieves, R. Gran, I. Ruiz Simo, F. Sánchez and M. J. Vicente Vacas, Nucl. Part. Phys. Proc. **273-275**, 1830-1835 (2016) doi:10.1016/j.nuclphysbps.2015.09.295 [arXiv:1411.7821 [hep-ph]].
- [41] P. A. Rodrigues *et al.* [MINERvA], Phys. Rev. Lett. **116**, 071802 (2016) doi:10.1103/PhysRevLett.116.071802 [arXiv:1511.05944 [hep-ex]].
- [42] A. Filkins *et al.* [MINERvA], Phys. Rev. D **101**, no.11, 112007 (2020) doi:10.1103/PhysRevD.101.112007 [arXiv:2002.12496 [hep-ex]].
- [43] A. M. Ankowski, O. Benhar, P. Coloma, P. Huber, C. M. Jen, C. Mariani, D. Meloni and E. Vagnoni, Phys. Rev. D **92**, no.7, 073014 (2015) doi:10.1103/PhysRevD.92.073014 [arXiv:1507.08560 [hep-ph]].
- [44] J. Singh, S. Nagu, J. Singh and R. B. Singh, Nucl. Phys. B **957**, 115103 (2020) doi:10.1016/j.nuclphysb.2020.115103 [arXiv:1909.10329 [nucl-th]].
- [45] S. Naaz, A. Yadav, J. Singh and R. B. Singh, Nucl. Phys. B **933**, 40-52 (2018) doi:10.1016/j.nuclphysb.2018.05.018 [arXiv:1804.02191 [hep-ph]].
- [46] C. Andreopoulos, A. Bell, D. Bhattacharya, F. Cavanna, J. Dobson, S. Dytman, H. Gallagher, P. Guzowski, R. Hatcher and P. Kehayias, *et al.* Nucl. Instrum. Meth. A **614**, 87-104 (2010) doi:10.1016/j.nima.2009.12.009 [arXiv:0905.2517 [hep-ph]].
- [47] G. J. Feldman and R. D. Cousins, Phys. Rev. D **57**, 3873-3889 (1998) doi:10.1103/PhysRevD.57.3873 [arXiv:physics/9711021 [physics.data-an]].
- [48] D. Drakoulakos *et al.* [MINERvA], [arXiv:hep-ex/0405002 [hep-ex]].
- [49] P. Adamson *et al.* [MINOS], Phys. Rev. D **77**, 072002 (2008) doi:10.1103/PhysRevD.77.072002 [arXiv:0711.0769 [hep-ex]].
- [50] H. Chen *et al.* [MicroBooNE], FERMILAB-PROPOSAL-0974.
- [51] C. Adams *et al.* [LBNE], [arXiv:1307.7335 [hep-ex]].

- [52] M. A. Acero *et al.* [NOvA and R. Group], Eur. Phys. J. C **80**, no.12, 1119 (2020) doi:10.1140/epjc/s10052-020-08577-5 [arXiv:2006.08727 [hep-ex]].
- [53] P. Adamson, K. Anderson, M. Andrews, R. Andrews, I. Anghel, D. Augustine, A. Aurisano, S. Avvakumov, D. S. Ayres and B. Baller, *et al.* Nucl. Instrum. Meth. A **806**, 279-306 (2016) doi:10.1016/j.nima.2015.08.063 [arXiv:1507.06690 [physics.acc-ph]].
- [54] K. Bora, D. Dutta and P. Ghoshal, Mod. Phys. Lett. A **30**, no.14, 1550066 (2015) doi:10.1142/S0217732315500662 [arXiv:1405.7482 [hep-ph]].
- [55] K. Bora and D. Dutta, J. Phys. Conf. Ser. **481**, 012019 (2014) doi:10.1088/1742-6596/481/1/012019 [arXiv:1209.1870 [hep-ph]].
- [56] K. Bora, G. Ghosh and D. Dutta, Adv. High Energy Phys. **2016**, 9496758 (2016) doi:10.1155/2016/9496758 [arXiv:1606.00554 [hep-ph]].
- [57] U. Mosel, O. Lalakulich and K. Gallmeister, Phys. Rev. D **89**, no.9, 093003 (2014) doi:10.1103/PhysRevD.89.093003 [arXiv:1402.0297 [nucl-th]].
- [58] A. Bodek, H. S. Budd and M. E. Christy, Eur. Phys. J. C **71**, 1726 (2011) doi:10.1140/epjc/s10052-011-1726-y [arXiv:1106.0340 [hep-ph]].
- [59] M. A. Acero *et al.* [NOvA and R. Group], Eur. Phys. J. C **80**, no.12, 1119 (2020) doi:10.1140/epjc/s10052-020-08577-5 [arXiv:2006.08727 [hep-ex]].
- [60] C. H. Llewellyn Smith, Phys. Rept. **3**, 261-379 (1972) doi:10.1016/0370-1573(72)90010-5.
- [61] A. Bodek and U. K. Yang, J. Phys. G **29**, 1899-1906 (2003) doi:10.1088/0954-3899/29/8/369 [arXiv:hep-ex/0210024 [hep-ex]].
- [62] T. Katori, AIP Conf. Proc. **1663**, no.1, 030001 (2015) doi:10.1063/1.4919465 [arXiv:1304.6014 [nucl-th]].
- [63] R. Bradford, A. Bodek, H. S. Budd and J. Arrington, Nucl. Phys. B Proc. Suppl. **159**, 127-132 (2006) doi:10.1016/j.nuclphysbps.2006.08.028 [arXiv:hep-ex/0602017 [hep-ex]].
- [64] S. Dytman, Acta Phys. Polon. B **40**, 2445-2460 (2009).
- [65] J. Nieves, I. Ruiz Simo and M. J. Vicente Vacas, Phys. Lett. B **707**, 72-75 (2012) doi:10.1016/j.physletb.2011.11.061 [arXiv:1106.5374 [hep-ph]].
- [66] M. A. Acero *et al.* [NOvA], [arXiv:2108.08219 [hep-ex]].
- [67] P. Adamson *et al.* [NOvA], Phys. Rev. D **93**, no.5, 051104 (2016) doi:10.1103/PhysRevD.93.051104 [arXiv:1601.05037 [hep-ex]].
- [68] D. P. Mendez Mendez, doi:10.2172/1579208
- [69] P. F. de Salas, D. V. Forero, S. Gariazzo, P. Martínez-Miravé, O. Mena, C. A. Ternes, M. Tórtola and J. W. F. Valle, JHEP **02**, 071 (2021) doi:10.1007/JHEP02(2021)071 [arXiv:2006.11237 [hep-ph]].
- [70] D. S. Pershey, doi:10.2172/1484186.
- [71] T. Nosek [NOvA], [arXiv:1905.09109 [hep-ex]].